Seismic data decomposition into spectral components using regularized nonstationary autoregression[a]

[a]Published in Geophysics, 78, no. 6, O69-O76, (2013)

Sergey Fomel

ABSTRACT

Seismic data can be decomposed into nonstationary spectral components with smoothly variable frequencies and smoothly variable amplitudes. To estimate local frequencies, I use a nonstationary version of Prony's spectral analysis method defined with the help of regularized nonstationary autoregression (RNAR). To estimate local amplitudes of different components, I fit their sum to the data using regularized nonstationary regression (RNR). Shaping regularization ensures stability of the estimation process and provides controls on smoothness of the estimated parameters. Potential applications of the proposed technique include noise attenuation, seismic data compression, and seismic data regularization.

INTRODUCTION

Decomposing data into components has an immediate application in noise-attenuation problems in cases where signal and noise correspond to different components. The classic Fourier transform, Radon transform (Gardner and Lu, 1991), wavelet transform (Mallat, 2009), curvelet frame (Herrmann and Hennenfent, 2008), and seislet transform and frame (Fomel and Liu, 2010) are some examples of possible decompositions applicable to seismic data. A fundamental characteristic of seismic data is non-stationarity. In 1D (time dimension), seismic data are nonstationary because of wave-attenuation effects. In 2D and 3D (time and space dimensions), non-stationarity is manifested by variable slopes of seismic events. The nonstationary character of seismic data can be captured by EMD (empirical mode decomposition) proposed by Huang et al. (1998). EMD has found a number of important applications in seismic data analysis (Magrin-Chagnolleau and Baraniuk, 1999; Battista et al., 2007; Bekara and van der Baan, 2009; Han and van der Baan, 2013). However, it remains "empirical" because its properties are not fully understood. Daubechies et al. (2011) recently proposed an EMD-like decomposition using the continuous wavelet transform and *synchrosqueezing* (Daubechies and Maes, 1996). Synchrosqueezing improves the analysis but remains an indirect method when it comes to extracting spectral attributes (Herrera et al., 2013).

In this paper, I develop an efficient decomposition algorithm, which explicitly fits seismic data to a sum of oscillatory signals with smoothly varying frequencies and smoothly varying amplitudes. Such a decomposition is close in properties to the one generated by EMD but with explicit controls on the frequencies and amplitudes of different components and on their smoothness. Recently, Hou and Shi (2011, 2013) developed an explicit data-adaptive decomposition based on matching-pursuit sparse optimization, an accurate but computationally expensive method. To implement a faster approach, I adopt regularized nonstationary regression, or RNR (Fomel, 2009), a general method for fitting data to a set of basis functions with nonstationary coefficients. RNR was previously applied to time-frequency decomposition over a set of regularly sampled frequencies (Liu and Fomel, 2013). When the input signal is fitted to shifted versions of itself, RNR turns into regularized nonstationary autoregression, or RNAR, and is related to adaptive prediction-error filtering. RNAR was previously applied to data regularization (Liu and Fomel, 2011) and noise removal (Liu et al., 2012; Liu and Chen, 2013). In this paper, I use it for spectral analysis and estimating different frequencies present in the data using a nonstationary extension of Prony's method of autoregressive spectral analysis (Marple, 1987; Bath, 1995). After the frequencies have been identified, I use RNR to determine local, smoothly-varying amplitudes of different components.

The paper opens with a brief review of RNR and RNAR and explains an extension of Prony's method to the nonstationary case. Next, I use simple synthetic and field-data examples to illustrate performance of the proposed technique.

REGULARIZED NONSTATIONARY REGRESSION

Regularized nonstationary regression (Fomel, 2009) is based on the following simple model. Let $d(\mathbf{x})$ represent the data as a function of data coordinates $\mathbf{x}$, and $b_n(\mathbf{x})$, $n = 1, 2, \ldots, N$, represent a collection of basis functions. The goal of *stationary* regression is to estimate coefficients a_n, $n = 1, 2, \ldots, N$ such that the prediction error

$$e(\mathbf{x}) = d(\mathbf{x}) - \sum_{n=1}^{N} a_n \, b_n(\mathbf{x}) \tag{1}$$

is minimized in the least-squares sense. In the case of regularized *nonstationary* regression (RNR), the coefficients become variable,

$$\hat{e}(\mathbf{x}) = d(\mathbf{x}) - \sum_{n=1}^{N} \hat{a}_n(\mathbf{x}) \, b_n(\mathbf{x}) \; . \tag{2}$$

The problem in this case is underdetermined but can be constrained by regularization (Engl et al., 1996). I use shaping regularization (Fomel, 2007) to implement an explicit control on the resolution and variability of regression coefficients. Shaping regularization applied to RNR amounts to linear inversion,

$$\mathbf{a} = \mathbf{M}^{-1} \, \mathbf{c} \; , \tag{3}$$

where $\mathbf{a}$ is a vector composed of $\hat{a}_n(\mathbf{x})$, the elements of vector $\mathbf{c}$ are

$$c_i(\mathbf{x}) = \mathbf{S}\left[b_i^*(\mathbf{x})\, d(\mathbf{x})\right] \ , \tag{4}$$

the elements of matrix $\mathbf{M}$ are

$$M_{ij}(\mathbf{x}) = \lambda^2\, \delta_{ij} + \mathbf{S}\left[b_i^*(\mathbf{x})\, b_j(\mathbf{x}) - \lambda^2\, \delta_{ij}\right] \ , \tag{5}$$

λ is a scaling coefficient, and $\mathbf{S}$ represents a shaping (typically smoothing) operator. When inversion in equation 3 is implemented by an iterative method, such as conjugate gradients, strong smoothing makes $\mathbf{M}$ close to identity and easier (taking less iterations) to invert, whereas weaker smoothing slows down the inversion but allows for more details in the solution. This intuitively logical behavior distinguishes shaping regularization from alternative methods (Fomel, 2009).

Regularized nonstationary autoregression (RNAR) corresponds to the case of basis functions being causal translations of the input data itself. In 1D, with $\mathbf{x} = t$, this condition implies $b_n(t) = d(t - n\,\Delta t)$.

AUTOREGRESSIVE SPECTRAL ANALYSIS

Prony's method of data analysis was developed originally for representing a noiseless signal as a sum of exponential components (Prony, 1795). It was extended later to noisy signals, complex exponentials, and spectral analysis (Pisarenko, 1973; Marple, 1987; Bath, 1995; Beylkin and Monzón, 2005). The basic idea follows from the fundamental property of exponential functions: $e^{\alpha\,(t+\Delta t)} = e^{\alpha\, t}\, e^{\alpha\, \Delta t}$. In signal-processing terms, it implies that a time sequence $d(t) = A\, e^{\alpha\, t}$ (with real or complex α) is predictable by a two-point prediction-error filter $\left(1, -e^{\alpha\, \Delta t}\right)$, or, in the Z-transform notation,

$$F_0(Z) = 1 - Z/Z_0 \ , \tag{6}$$

where $Z_0 = e^{-\alpha\, \Delta t}$. If the signal is composed of multiple exponentials,

$$d(t) \approx \sum_{n=1}^{N} A_n\, e^{\alpha_n\, t} \ , \tag{7}$$

they can be predicted simultaneously by using a convolution of several two-point prediction-error filters:

$$\begin{aligned} F(Z) &= (1 - Z/Z_1)\,(1 - Z/Z_2)\,\cdots\,(1 - Z/Z_N) \\ &= 1 + a_1\, Z + a_2\, Z^2 + \cdots + a_n\, Z^N \ , \end{aligned} \tag{8}$$

where $Z_n = e^{-\alpha_n\, \Delta t}$. This observation suggests the following three-step algorithm:

1. Estimate a prediction-error filter from the data by determining filter coefficients $a_1, a_2, \ldots, a_N$ from the least-squares minimization of

$$e(t) = d(t) - \sum_{n=1}^{N} a_n\, d(t - n\,\Delta t) \ . \tag{9}$$

2. Writing the filter as a Z polynomial (equation 8), find its complex roots $Z_1, Z_2, \ldots, Z_N$. The exponential factors $\alpha_1, \alpha_2, \ldots, \alpha_N$ are determined then as

$$\alpha_n = -\ln(Z_n)/\Delta t \ . \tag{10}$$

3. Estimate amplitudes $A_1, A_2, \ldots, A_N$ of different components in equation 7 by linear least-squares fitting.

Prony's method can be applied in sliding windows, which was a technique developed by Russian geophysicists (Gritsenko et al., 2001; Mitrofanov and Priimenko, 2011) for identifying low-frequency seismic anomalies (Mitrofanov et al., 1998). I propose to extend it to smoothly nonstationary analysis by applying the following modifications:

1. Using RNAR, the filter coefficients a_n become smoothly-varying functions of time $\hat{a}_n(t)$, which allows the filter to adapt to nonstationary changes in the input data.

2. At each instance of time, roots of the corresponding Z polynomial also become functions of time $\hat{Z}_n(t)$. I apply a robust, eigenvalue-based algorithm for root finding (Toh and Trefethen, 1994). The instantaneous frequency of different components $f_n(t)$ is determined directly from the phase of different roots:

$$f_n(t) = -Re\left[\arg\left(\frac{\hat{Z}_n(t)}{2\pi\,\Delta t}\right)\right] \ . \tag{11}$$

3. Finally, using RNR, I estimate smoothly-varying amplitudes of different components $\hat{A}_n(t)$.

The nonstationary decomposition model for a complex signal $d(t)$ is thus

$$d(t) \approx \sum_{n=1}^{N} d_n(t) \ , \quad \text{where} \quad d_n(t) = \hat{A}_n(t)\, e^{i\,\phi_n(t)} \tag{12}$$

and the local phase $\phi_n(t)$ corresponds to time integration of the instantaneous frequency determined in Step 2:

$$\phi_n(t) = 2\pi \int_0^t f_n(\tau) d\tau \ . \tag{13}$$

For ease of analysis, real signals can be transformed to the complex domain by using analytical traces (Taner et al., 1979).

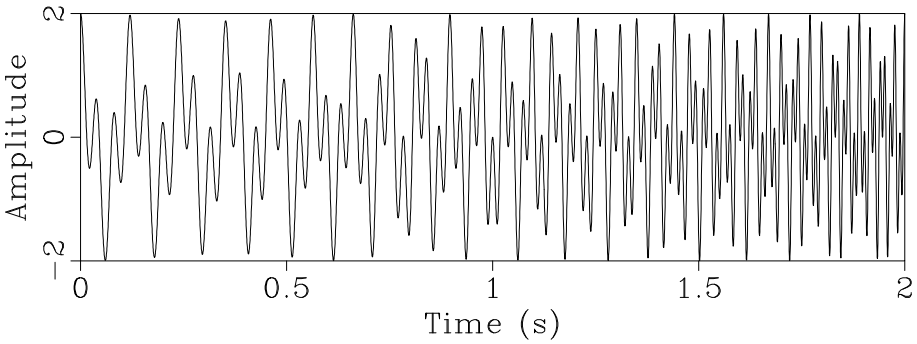

a

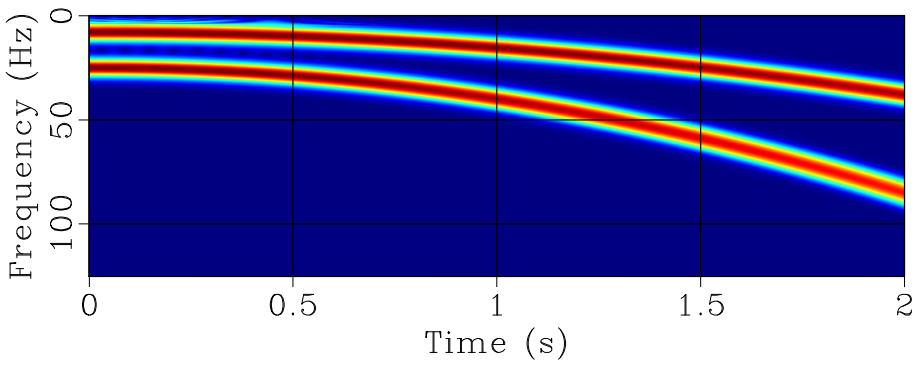

b

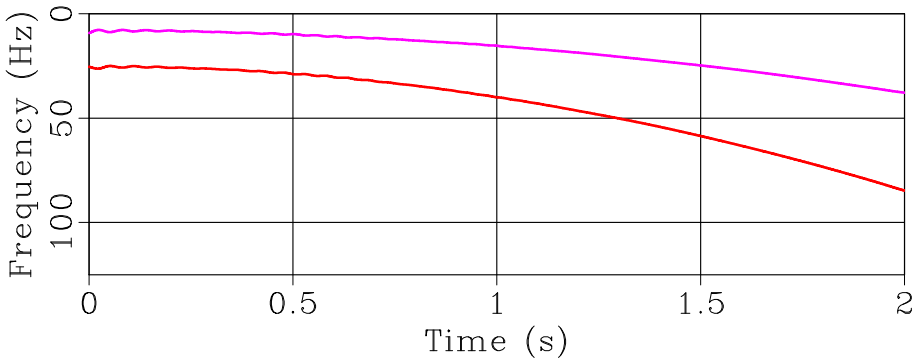

c

Figure 1: (a) Test signal from Liu et al. (2011) composed of two variable-frequency components. (b) Time-frequency decomposition. (c) Instantaneous frequencies estimated by RNAR.

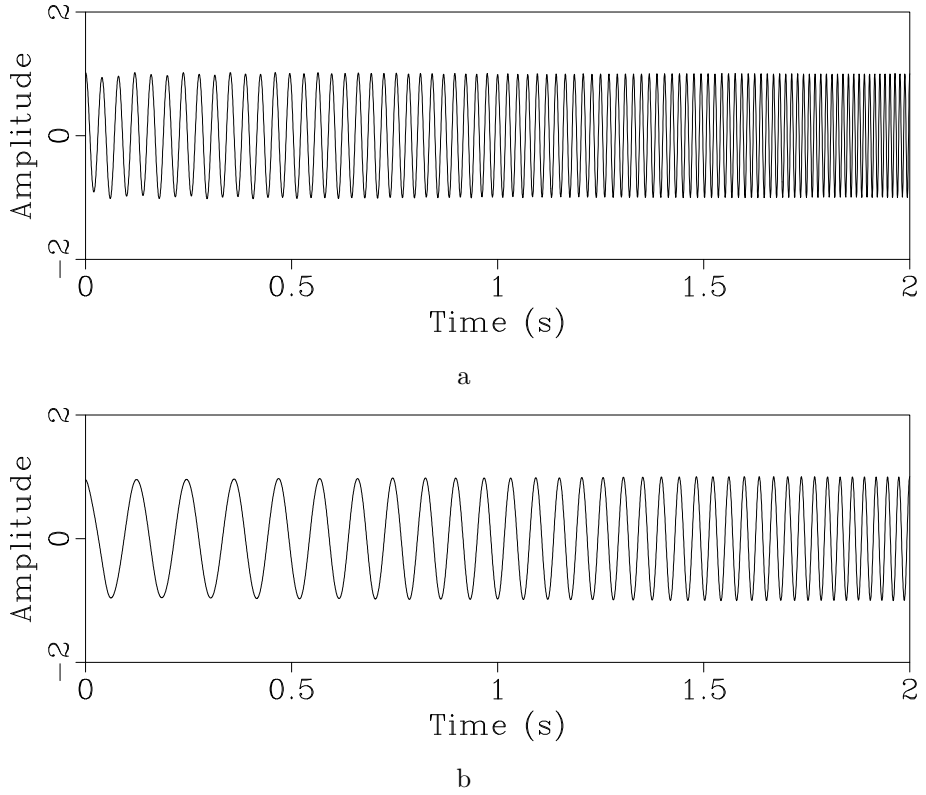

Figure 2: Decomposition of the signal from Figure 1a into two spectral components using RNR.

Benchmark tests

Figure 1a shows a benchmark signal from Liu et al. (2011), which consists of two nonstationary components with smoothly varying (parabolic) frequencies. The corresponding time-frequency analysis over a range of regularly sampled frequencies is shown in Figure 1b. Two instantaneous frequencies were extracted at Step 2 of the algorithm from a time-varying, three-point prediction-error filter (Figure 1c). They correspond precisely to the two components present in the synthetic signal. Finally, Step 3 separates these components (Figure 2.)

The next benchmark example is taken from Herrera et al. (2013). Figure 3a shows the input signal, which is composed of several components with variable frequencies. The components can be identified in the time-frequency decomposition analysis (Figure 3b) generated with the method of Liu et al. (2011). More directly, they are extracted using RNAR (the method of this paper), with the output shown in Figure 3c. Fitting a sum of different components to the data by RNR, we can estimate their respective amplitudes. The output is shown in Figure 4. For comparison, I show the output of EMD (empirical mode decomposition) in Figure 5. For robustness, I used EEMD (ensemble EMD) suggested by Wu and Huang (2009). Although EEMD succeeds in separating the signal into components with variable frequencies, the individual components are not as meaningful as those identified by RNAR.

The third benchmark test is taken from Hou and Shi (2013). The signal in this case (Figure 6a) consists of three components with variable frequencies and amplitudes (Figure 7). RNAR correctly identifies the three components (Figure 6c) that are also visible on the time-frequency plot (Figure 6b). Next, RNR extracts the three components (Figure 8) by fitting their sum to the data (Figure 9) and adjusting the amplitudes. The sparse inversion algorithm proposed by Hou and Shi (2013) achieves a more accurate result in this case but at a much higher computational cost.

Discussion

The cost of the proposed decomposition is $O\left(N\, N_t\, N_{iter}\right)$, where N is the number of components, N_t is the number of time samples, and N_{iter} is the number of conjugate-gradient iterations for shaping regularization (typically between 10 and 100). This is significantly faster than the $O\left(N_t^2\, N_{iter}\right)$ cost of time-frequency decomposition for a regularly sampled range of frequencies.

Although the examples of this paper use only 1D analysis, the proposed technique is also directly applicable to analyzing variable slopes of 2D and 3D seismic events, where the analysis applies to different frequency slices in the f-x domain (Canales, 1984; Spitz, 1999, 2000; Liu et al., 2012; Liu and Chen, 2013).

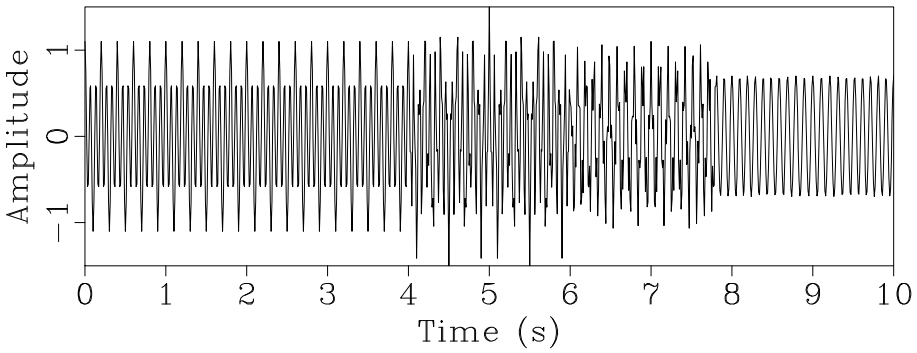

a

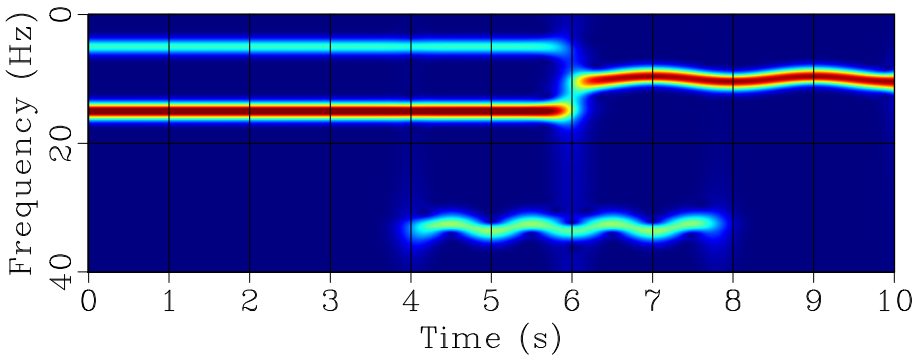

b

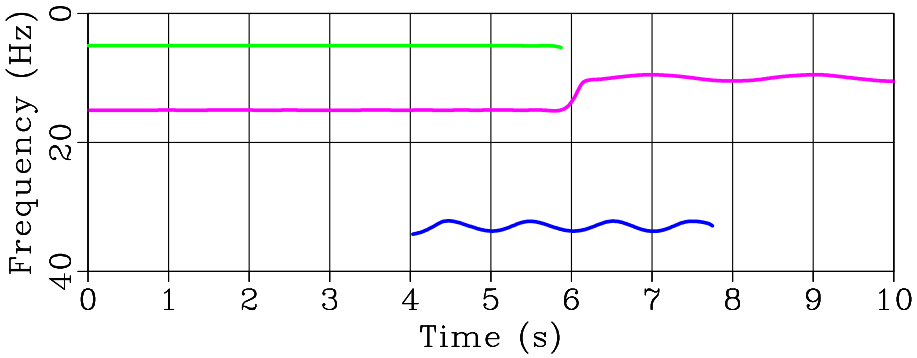

c

Figure 3: (a) Test signal from Herrera et al. (2013) composed of several variable-frequency components. (b) Time-frequency decomposition. (c) Instantaneous frequencies estimated by RNAR.

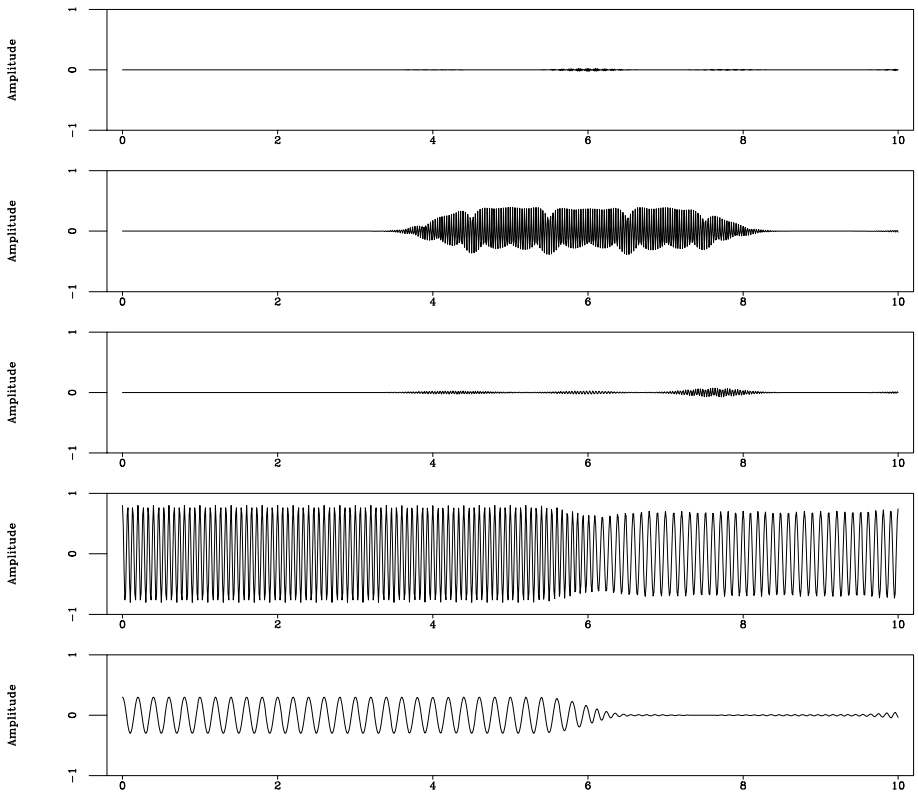

Figure 4: Decomposition of the signal from Figure 3a into spectral components using RNR. The components are sorted in the order of decreasing frequency.

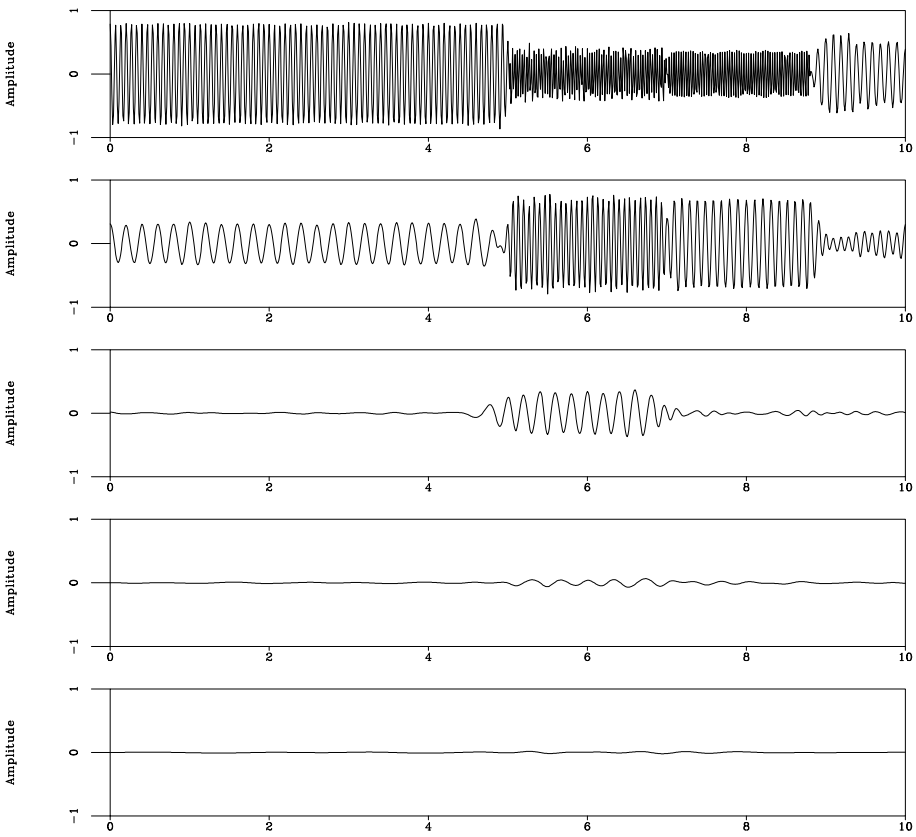

Figure 5: Decomposition of the signal from Figure 3a into intrinsic mode functions using EMD. Compare with Figure 4.

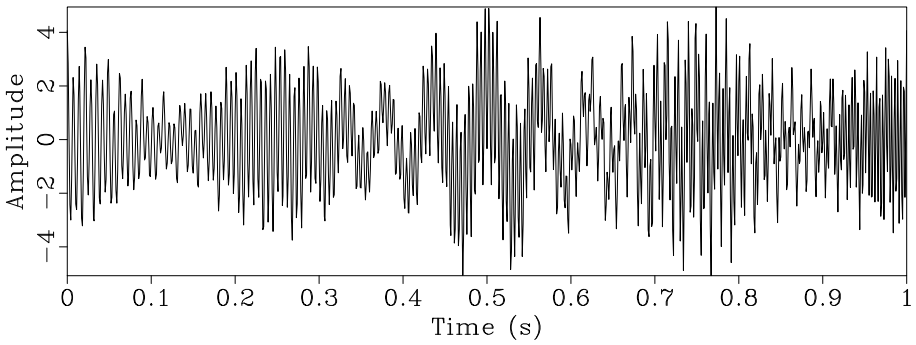

a

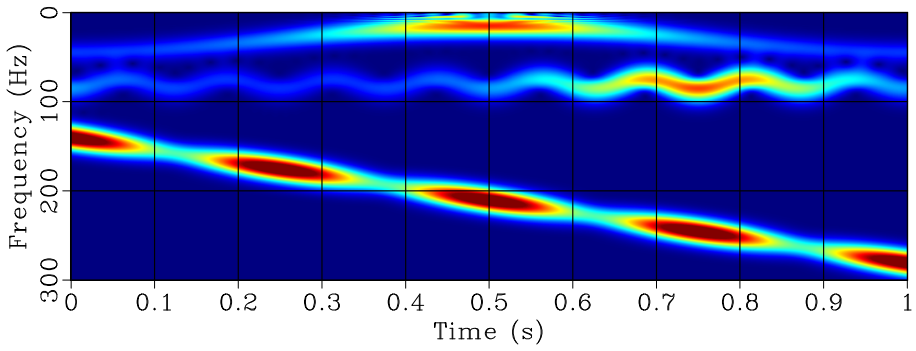

b

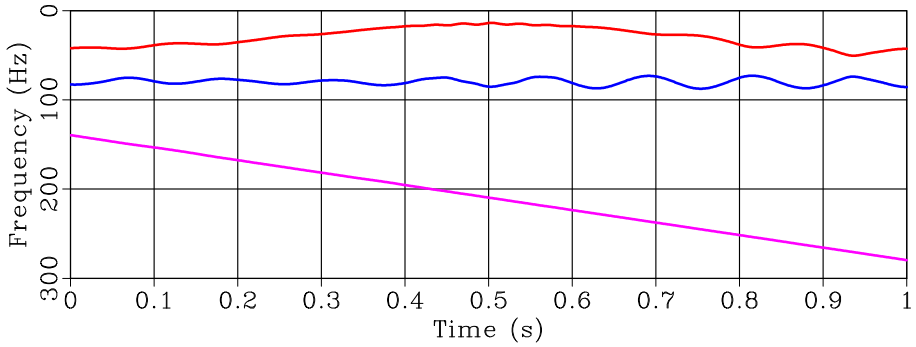

c

Figure 6: (a) Test signal from Hou and Shi (2013) composed of several variable-frequency and variable-amplitude components. (b) Time-frequency decomposition. (c) Instantaneous frequencies estimated by RNAR.

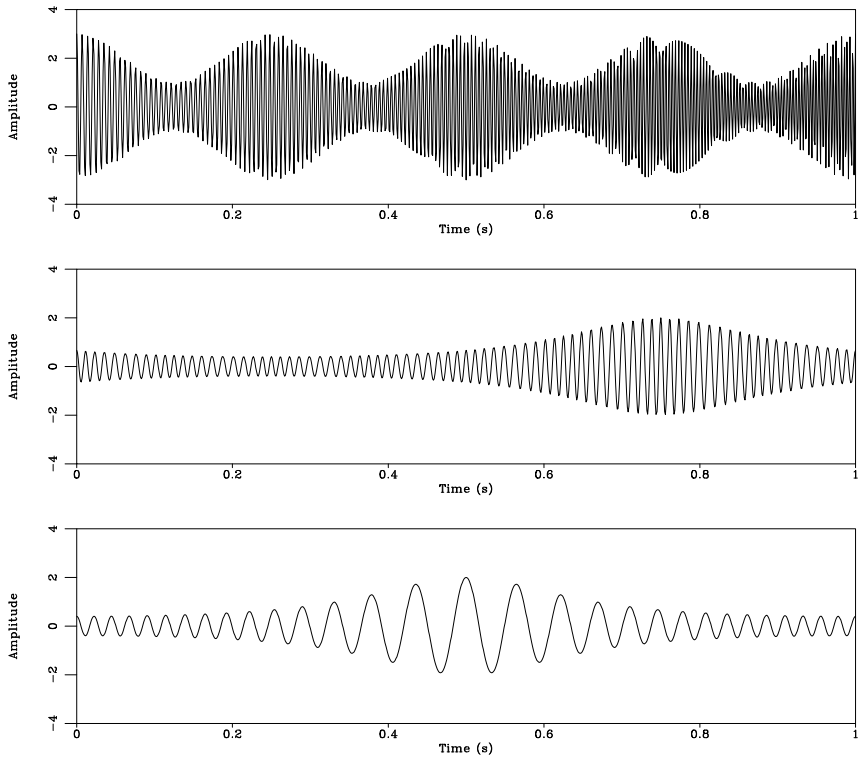

Figure 7: Signal components making the signal in Figure 6a.

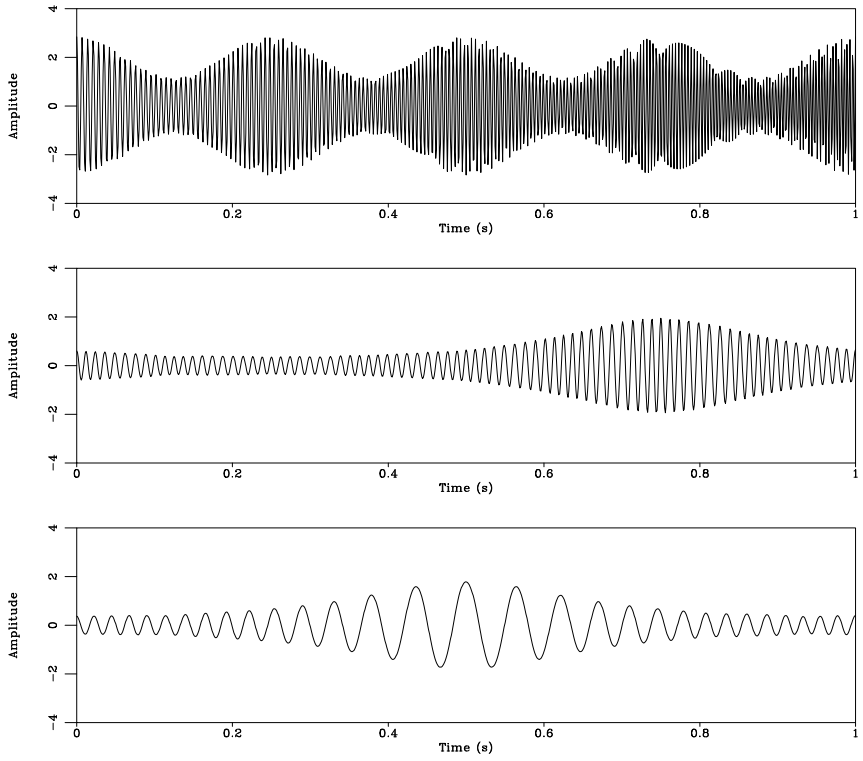

Figure 8: Decomposition of the signal from Figure 6a into spectral components using RNR.

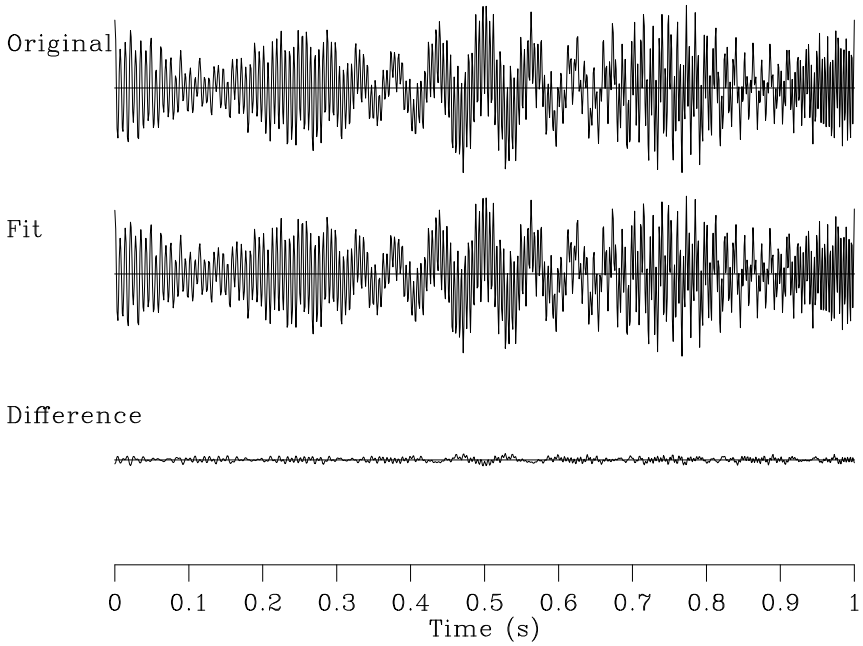

Figure 9: Fitting the signal from Figure 6a with the sum of three components shown in Figure 8.

EXAMPLES

To illustrate performance of the proposed approach in field-data applications, I first use a simple 1D example: a single seismic trace from a marine survey. Figure 10 shows the input trace and the output of RNAR, with a five-point adaptive prediction-error filter. The four variable instantaneous frequencies extracted from the roots of the filter are shown in Figure 11. They correspond to four different spectral components extracted from the data in Step 3 (Figure 12.) Surprisingly, only four components with smoothly varying frequencies and amplitudes are sufficient to describe a significant portion of the signal, including the effect of attenuating frequencies at later times (Figure 13.)

The second example is a 2D section from a land seismic survey (Figure 14a), analyzed previously by Fomel (2007) and Liu and Fomel (2013). I choose a three-point prediction-error filter to highlight the two most significant data components. The fitting error is shown in Figure 15 and contains mostly random noise. The two estimated spectral components are shown in Figure 16, with the corresponding instantaneous frequencies $f_n)t)$ shown in Figure 17. The corresponding amplitudes $|\hat{A}_n(t)|$ are shown in Figure 18. Comparing frequency and amplitude attributes from different components, a low-frequency anomaly (a zone of attenuated high frequencies) in the top-left part of the section becomes apparent. This anomaly might indicate presence of gas (Castagna et al., 2003).

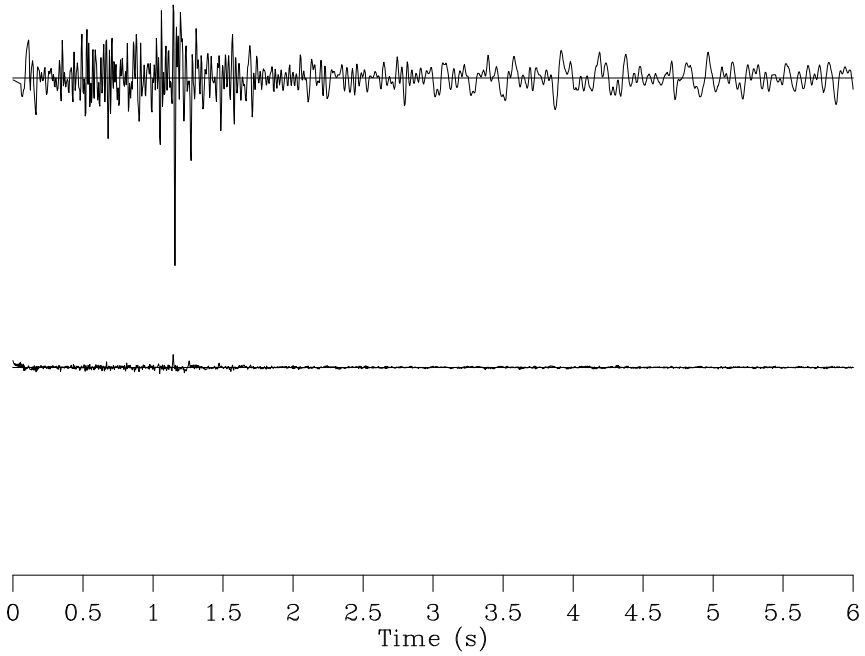

Figure 10: Seismic trace and residual after adaptive prediction-error filtering with RNAR.

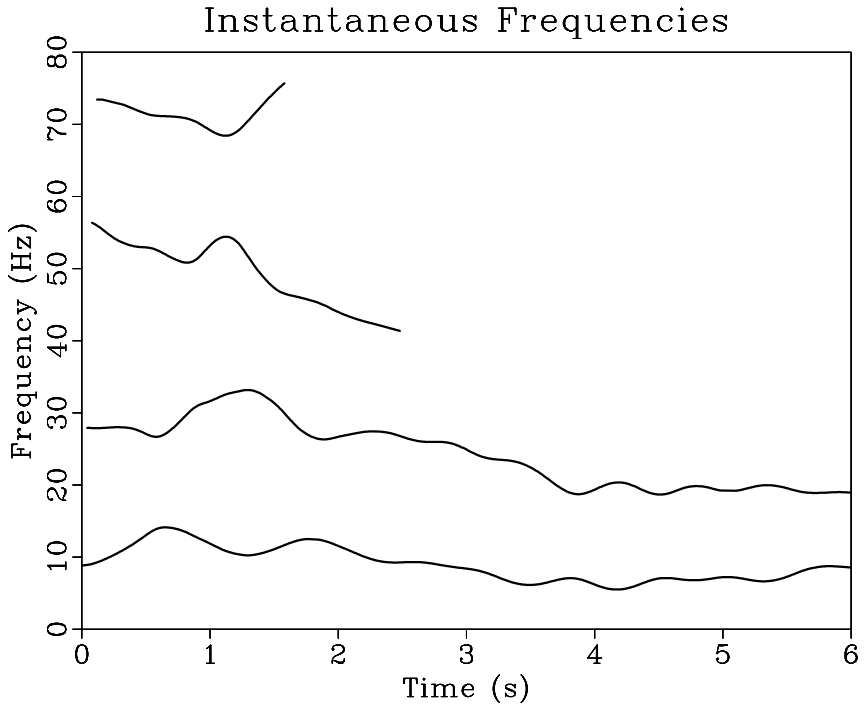

Figure 11: Instantaneous frequencies of four components extracted from seismic trace in Figure 10 using RNAR.

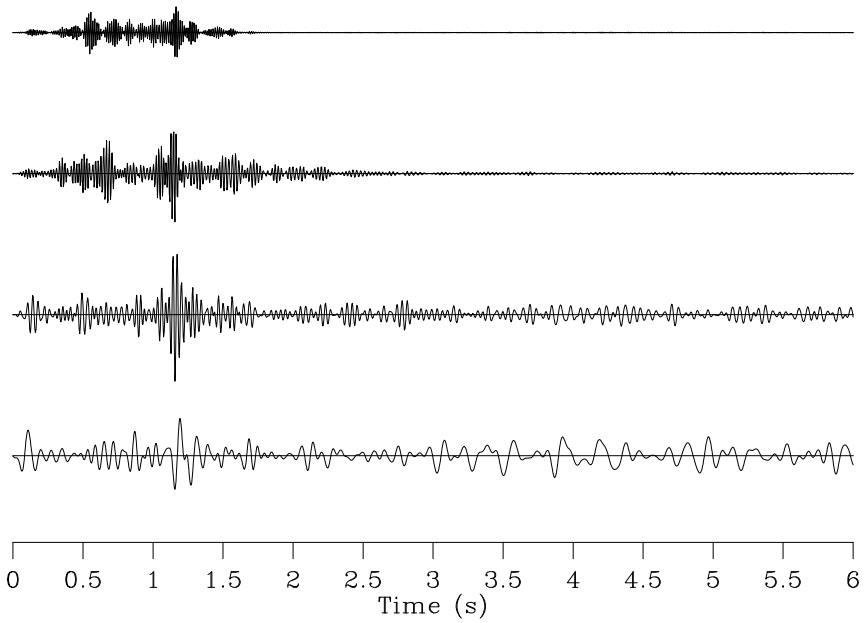

Figure 12: Four nonstationary spectral components corresponding to frequencies in Figure 11.

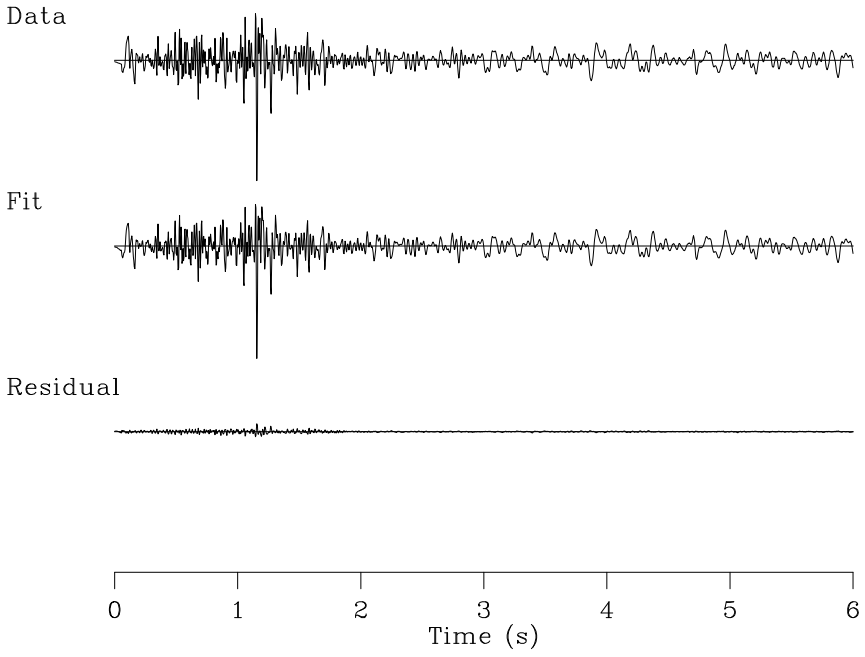

Figure 13: Fitting input seismic trace with sum of four spectral components shown in Figure 12.

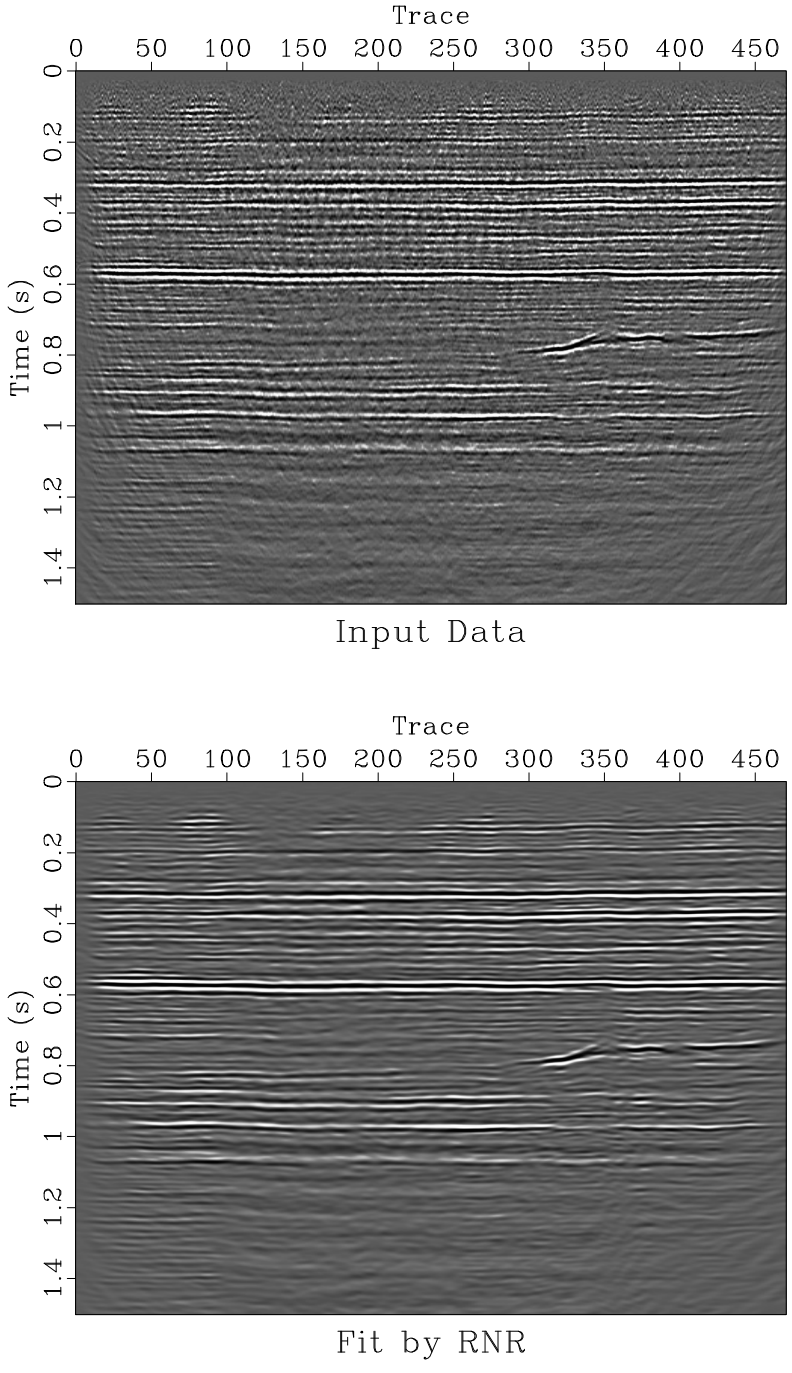

Figure 14: (a) 2D seismic data section. (b) Result of fitting data with two components shown in Figure 16.

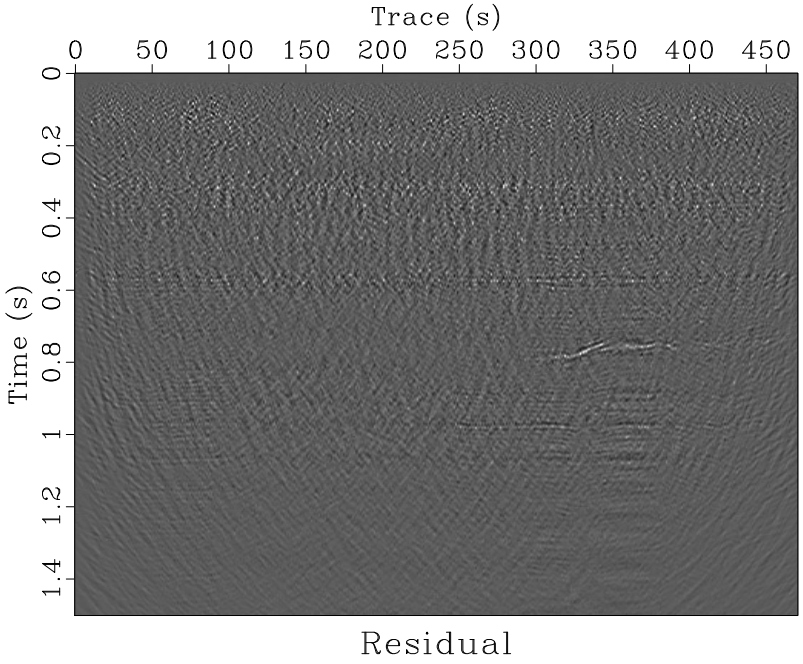

Figure 15: Residual error after fitting seismic data from Figure 14 with two components shown in Figure 16.

CONCLUSIONS

I have presented a constructive approach to decomposing seismic data into spectral components with smoothly variable frequencies and smoothly variable amplitudes. The output of the proposed algorithm is close to that of empirical model decomposition (EMD) and related techniques, such as the synchrosqueezing transform (SST), but with a more explicit control on parameters and more direct access to instantaneous-frequency and amplitude attributes. The main tool for the task is regularized nonstationary regression (RNR), which is applied twice: first to estimate local frequencies by autoregression (RNAR) and then to estimate local amplitudes. Although all examples shown in this paper use only 1D analysis, the proposed technique is also applicable to analyzing 2D or 3D variable-slope seismic events in the f-x domain. Potential applications may include noise attenuation, data compression, and data regularization.

ACKNOWLEDGMENTS

I would like to thank Sergey Gritsenko for teaching me Prony's method more than 20 years ago. I am also grateful to Yihua Cai, Yangkang Chen, Henry Herrera, Guochang Liu, Yang Liu, Karl Schleicher, Mirko van der Baan, and Lexing Ying for inspiring discussions.

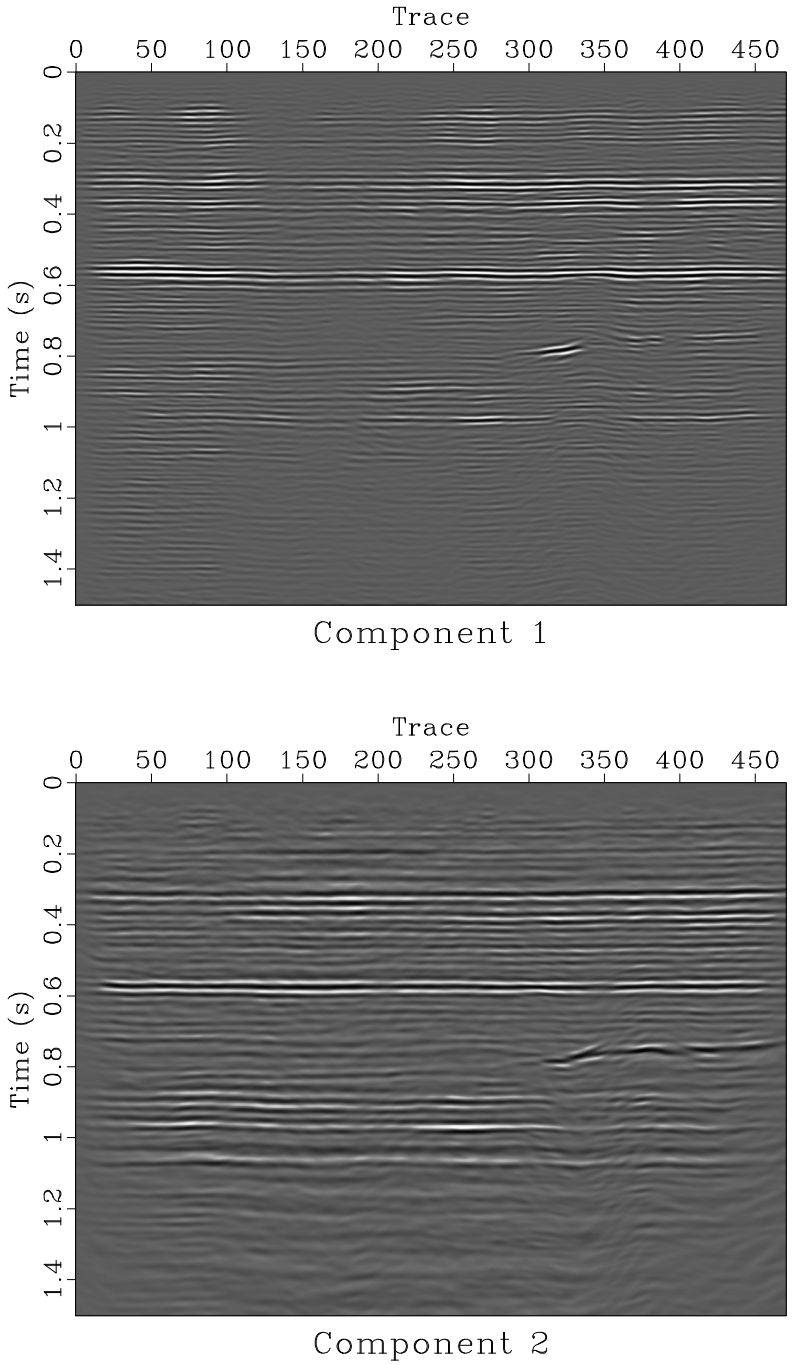

Figure 16: Two nonstationary spectral components: high-frequency (Component 1) and low-frequency (Component 2) estimated from the data shown in Figure 14a.

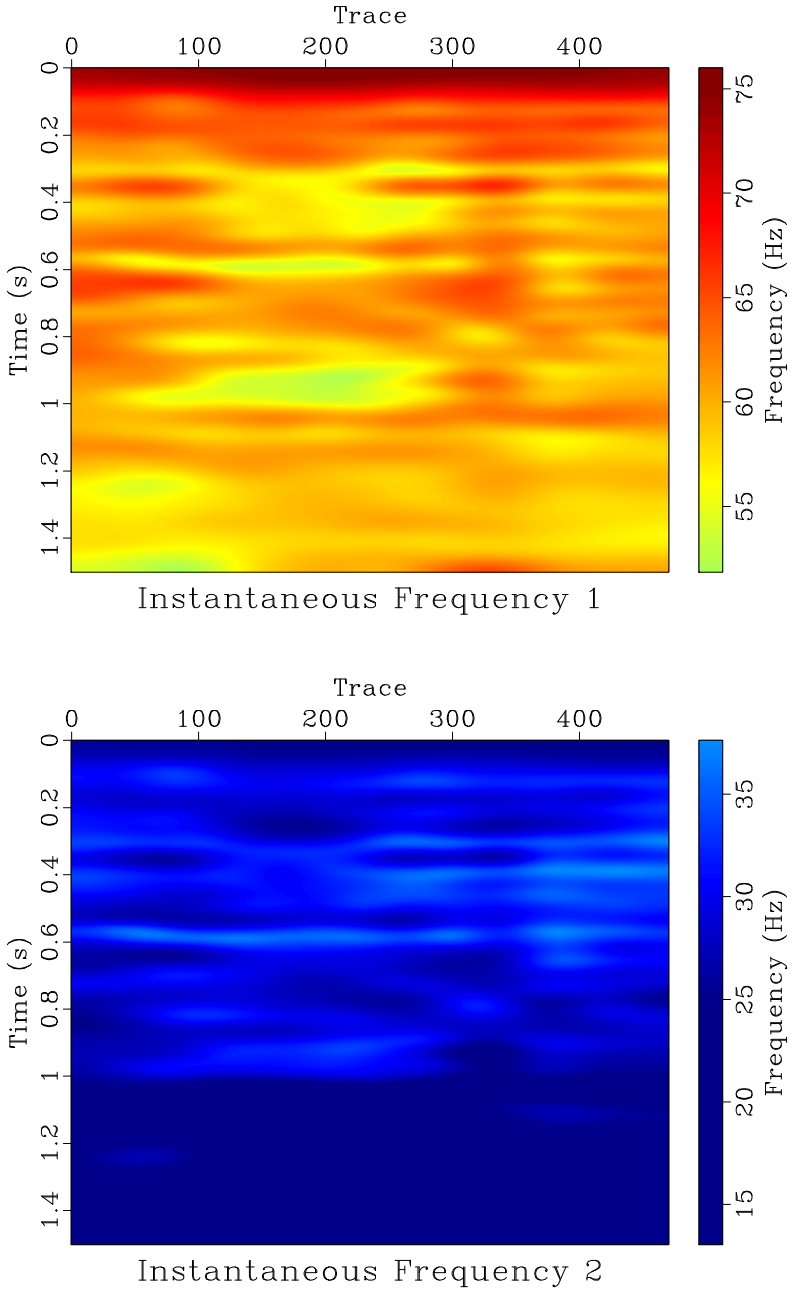

Figure 17: Instantaneous frequencies of high-frequency and low-frequency components from decomposition shown in Figure 16.

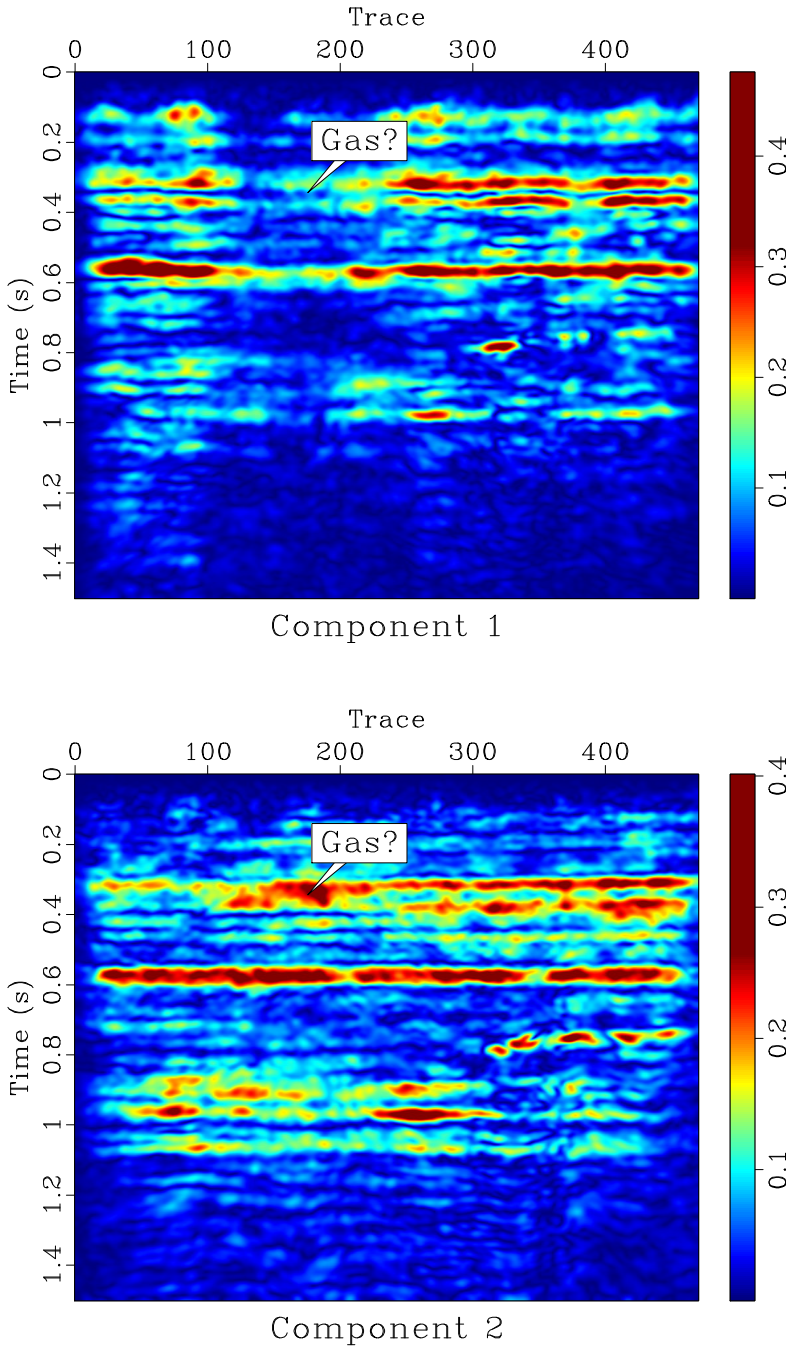

Figure 18: Amplitudes of high-frequency and low-frequency components from decomposition shown in Figure 16. The apparent attenuation of high frequencies in the top left part of the section may indicate presence of gas.

REFERENCES

Bath, M., 1995, Modern Spectral Analysis with Geophysical Applications: Soc. of Expl. Geophys. (Edited by Robert E. Wiley).

Battista, B. M., C. Knapp, T. McGee, and V. Goebel, 2007, Application of the empirical mode decomposition and Hilbert-Huang transform to seismic reflection data: Geophysics, **72**, H29–H37.

Bekara, M., and M. van der Baan, 2009, Random and coherent noise attenuation by empirical mode decomposition: Geophysics, **74**, V89–V98.

Beylkin, G., and L. Monzón, 2005, On approximation of functions by exponential sums: Applied and Computational Harmonic Analysis, **19**, 17–48.

Canales, L. L., 1984, Random noise reduction: 54th Ann. Internat. Mtg, Soc. of Expl. Geophys., Session:S10.1.

Castagna, J. P., S. Sun, and R. W. Siegfried, 2003, Instantaneous spectral analysis: Detection of low-frequency shadows associated with hydrocarbons: The Leading Edge, **22**, 120–127.

Daubechies, I., J. Lu, and H.-T. Wu, 2011, Synchrosqueezed wavelet transforms: An empirical mode decomposition-like tool: Applied and Computational Harmonic Analysis, **30**, 243–261.

Daubechies, I., and S. Maes, 1996, A nonlinear squeezing of the continuous wavelet transform based on auditory nerve models, *in* Wavelets in medicine and biology: CRC Press, 527–546.

Engl, H., M. Hanke, and A. Neubauer, 1996, Regularization of inverse problems: Kluwer Academic Publishers.

Fomel, S., 2007, Shaping regularization in geophysical-estimation problems: Geophysics, **72**, R29–R36.

———, 2009, Adaptive multiple subtraction using regularized nonstationary regression: Geophysics, **74**, V25–V33.

Fomel, S., and Y. Liu, 2010, Seislet transform and seislet frame: Geophysics, **75**, V25–V38.

Gardner, G. H. F., and L. Lu, eds., 1991, Slant-stack processing: Society of Exploration Geophysicists. Issue 14 of Geophysics reprint series.

Gritsenko, S. A., S. Fomel, and V. S. Chernyak, 2001, Filtering using Prony's method: Geofizika, 24–26 (in Russian).

Han, J., and M. van der Baan, 2013, Empirical mode decomposition for seismic time-frequency analysis: Geophysics, **78**, O9–O19.

Herrera, R. H., J.-B. Tary, and M. van der Baan, 2013, Time-frequency representation of microseismic signals using the synchrosqueezing transform, *in* Geoconvention: Can. Soc. Expl. Geophys.

Herrmann, F. J., and G. Hennenfent, 2008, Non-parametric seismic data recovery with curvelet frames: Geophysical Journal International, **173**, 233–248.

Hou, T. Y., and Z. Shi, 2011, Adaptive data analysis via sparse time-frequency representation: Advances in Adaptive Data Analysis, **3**, 1–28.

———, 2013, Data-driven time-frequency analysis: Applied and Computational Harmonic Analysis, **35**, 284308.

Huang, N. E., Z. Shen, S. R. Long, M. C. Wu, H. H. Shih, Q. Zheng, N.-C. Yen, C. C. Tung, and H. H. Liu, 1998, The empirical mode decomposition and the Hilbert spectrum for nonlinear and non-stationary time series analysis: Proceeding of the Royal Society of London Series A, **454**, 903–995.

Liu, G., and X. Chen, 2013, Noncausal f-x-y regularized nonstationary prediction filtering for random noise attenuation on 3D seismic data: Journal of Applied Geophysics, **93**, 60–66.

Liu, G., X. Chen, J. Du, and K. Wu, 2012, Random noise attenuation using f-x regularized nonstationary autoregression: Geophysics, **77**, V61–V69.

Liu, G., S. Fomel, and X. Chen, 2011, Time-frequency analysis of seismic data using local attributes: Geophysics, **76**, P23–P34.

Liu, Y., and S. Fomel, 2011, Seismic data interpolation beyond aliasing using regularized nonstationary autoregression: Geophysics, **76**, V69–V77.

———, 2013, Seismic data analysis using local time-frequency decomposition: Geophysical Prospecting, **61**, 516–525.

Magrin-Chagnolleau, I., and R. Baraniuk, 1999, Empirical mode decomposition based frequency attributes: 69th Ann. Internat. Mtg, Soc. of Expl. Geophys., 1949–1952.

Mallat, S., 2009, A wavelet tour of signal processing: The sparse way: Academic Press.

Marple, S. L., 1987, Digital spectral analysis with applications: Prentice-Hall.

Mitrofanov, G., Z. Zhan, and J. Cai, 1998, Using of the Proni transform of Chinese seismic data: 68th Ann. Internat. Mtg, Soc. of Expl. Geophys., 1157–1159.

Mitrofanov, G. M., and V. I. Priimenko, 2011, Prony filtration of seismic data: theoretical background: Revista Brasileira de Geofísica, **29**.

Pisarenko, V. F., 1973, The retrieval of harmonics from a covariance function: Journal of the Royal Astronomical Society, **33**, 347–366.

Prony, R., 1795, Essai expérimental et analytique: Annuaire de l'École Polytechnique, **1**, 24.

Spitz, S., 1999, Pattern recognition, spatial predictability, and subtraction of multiple events: The Leading Edge, **18**, 55–58.

———, 2000, Model-based subtraction of multiple events in the frequency-space domain: 70th Ann. Internat. Mtg, Soc. of Expl. Geophys., 1969–1972.

Taner, M. T., F. Koehler, and R. E. Sheriff, 1979, Complex seismic trace analysis: Geophysics, **44**, 1041–1063. (Errata in GEO-44-11-1896; Discussion in GEO-45-12-1877-1878; Reply in GEO-45-12-1878-1878).

Toh, K., and L. Trefethen, 1994, Pseudozeros of polynomials and pseudospectra of companion matrices: Mathematik, **68**, 403–425.

Wu, Z., and N. E. Huang, 2009, Ensemble empirical mode decomposition: a noise-assisted data analysis method: Advances in Adaptive Data Analysis, **1**, 1–41.